INTERSECTION BASED REGISTRATION OF SLICE STACKS TO FORM 3D IMAGES OF THE HUMAN FETAL BRAIN

K. Kim[1], M. Hansen[1,3], P. Habas[1], F. Rousseau[4], O. Glenn[2], A.J. Barkovich[2], C. Studholme[1]

[1]Biomedical Image Computing Group, Dept. of Radiology, University of California San Francisco, San Francisco CA, USA

[2]Department of Radiology, University of California San Francisco, San Francisco CA, USA

[3]Department of Informatics and Mathematical Modelling, Technical University of Denmark, Kgs. Lyngby, Denmark

[4]Centre National de la Recherche Scientifique, Universite Louis Pasteur, Brant, Illikirch, France

ABSTRACT

Clinical fetal MR imaging of the brain commonly makes use of fast 2D acquisitions of multiple sets of approximately orthogonal 2D slices. We and others have previously proposed an iterative slice-to-volume registration process to recover a geometrically consistent 3D image. However, these approaches depend on a 3D volume reconstruction step during the slice alignment. This is both computationally expensive and makes the convergence of the registration process poorly defined. In this paper our key contribution is a new approach which considers the collective alignment of all slices directly, via shared structure in their intersections, rather than to an estimated 3D volume. We derive an analytical expression for the gradient of the collective similarity of the slices along their intersections, with respect to the 3D location and orientation of each 2D slice. We include examples of the approach applied to simulated data and clinically acquired fetal images.

Index Terms— Image registration, 3D reconstruction, Magnetic resonanace imaging, Fetal brain, Motion compensation

1. INTRODUCTION

MRI is emerging as a powerful new clinical tool in the early detection of subtle structural abnormalities in the developing human fetal brain [1, 2]. It provides improved tissue contrast in comparison to ultrasound imaging. This enables the detection of a range of subtle features not visible on prenatal ultrasound, such as gyral and sulcal abnormalities [2–6]. The development of ultrafast 2D acquisition sequences has led to significant improvements in the clinical utility of fetal MRI [7, 8]. However, the slice acquisition time is still critical and has to be as short as possible to reduce the impact of fetal and maternal motion on the exam, since fetal MRI is often performed without sedation. As a result, sets of thick 2D slices are generally acquired in clinical studies, with motion commonly occurring between slices. Overall, the resulting image data is limited in its geometric integrity between slices due to motion, and in its through plane spatial resolution.

In previous work we proposed the first approach to using image registration to take clinically acquired 2D slice data and form a single high resolution 3D MR image [9, 10] from multiple orthogonal stacks. Similar approaches were later proposed by [11]. Both of these methods made use of a slice to volume reconstruction-registration process in order to refine the final image formed by sets of movement perturbed slice stacks. Critically this approach is limited computationally and algorithmically by the reconstruction step. The initial reconstruction is blurred by the misalignment of the individual slices, and a sharpening of the image is not guaranteed by the slice to volume registration.

In this paper we propose a new approach to the problem which considers the registration process directly in terms of the intersections of each pair of slices in the stacks. We derive a gradient based formulation of the improvement of the alignment of data in the intersection of every slice with every other slice.

2. METHOD

2.1. Algorithm

The proposed algorithm aligns three stacks of 2D slices, which are approximately orthogonal to one another. Each slice is assumed to undergo 3D rigid body motion, thus having 6 degrees of freedom.

Two slices drawn from two orthogonal stacks have an intersection, and each slice has its own intensity profile along this intersection. When the two slices are aligned, the profiles precisely match against each other. If they are not aligned, the difference of the profiles can be used to estimate the translation and rotation of one slice relative to the other when the gradients of the two images are available. This can be generalized to the case of multiple stacks. Given n_A, n_S, and n_C slices in the axial, sagittal, and coronal stacks, respectively, there are in total $N = n_A + n_S + n_C$ slices, and the stack set has as many as $n_A n_S + n_S n_C + n_C n_A$ inter-stack intersections. The three translation and three rotational degrees of freedom of each slice are parametrized by

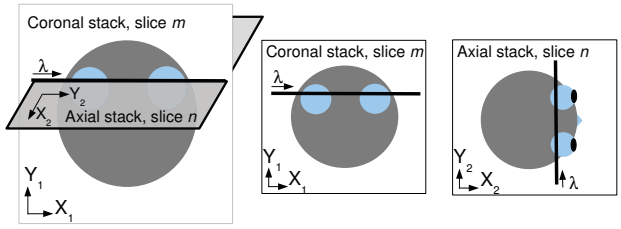

Fig. 1. Any two slices from two orthogonal stacks have intersection against each other. When a profile is taken from each image along this intersection, two profiles from the two images match precisely if the slices are aligned. The intersection is parameterized by λ, and the similarity measure can be evaluated as a function of λ. In this way, the gradient of the energy function can be directly calculated by the spatial gradient of the images.

$\theta = [x, y, z, r_x, r_y, r_z]^\top$. The global energy function is defined by the sum of dissimilarity measures of all intersection profiles between two orthogonal slices.

$$E(\Theta) = \sum_{i=1}^{N} \sum_{j \in S_i} \mathcal{D}_{ij} \tag{1}$$

where the dissimilarity measure $\mathcal{D}_{ij}$ is defined between two intersecting slices i and j, drawn from two orthogonal stacks,

$$\mathcal{D}_{ij} \equiv \mathcal{D}_{ij}(I_i, I_j; \theta_i, \theta_j) \tag{2}$$

and S_i, I_i, Θ represent the set of slices from the stacks orthogonal to the i-th slice, the i-th slice image, and the set of all the motion parameters of the slices in the stack set, namely, $\Theta = [\theta_1^\top \cdots \theta_N^\top]^\top$.

In order to minimize the energy function in (1), any optimization scheme can be used, such as Newton based or gradient descent methods.

2.2. Implementation

In this work, the mean of squared difference (MSD) was used for the dissimilarity measure,

$$\mathcal{D}_{ij} \equiv \frac{1}{|I_i \bigcap I_j|} \times \int_{I_i \bigcap I_j} ||I_i(\mathbf{x}_{ij}(\lambda; \theta_i, \theta_j)) - I_j(\mathbf{x}_{ji}(\lambda; \theta_j, \theta_i))||^2 d\lambda, \tag{3}$$

where the vector $\mathbf{x}_{ij}(\lambda; \Theta)$ is a position vector in the i-th image, along the intersection between the i-th and j-th images, one dimensionally parameterized by λ. We define a lexicographical representation of the intensity difference on all the intersections, $D = D(\Theta)$. Using this representation, (1) is rewritten simply by $E(\Theta) = ||D(\Theta)||^2$.

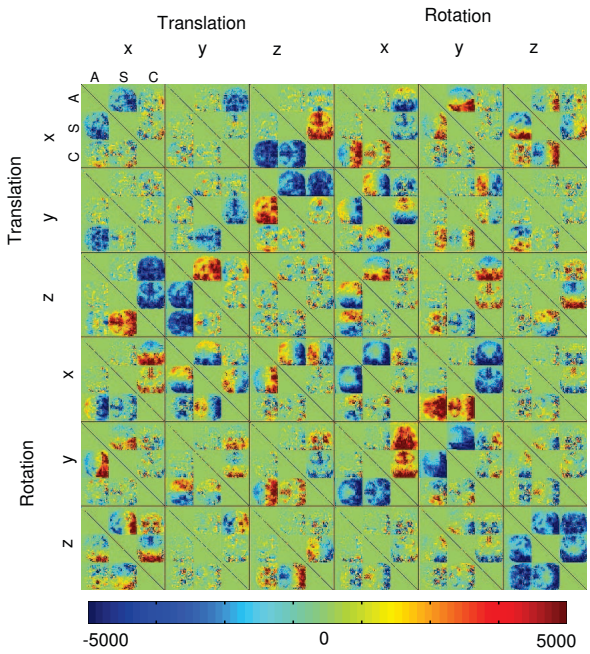

Fig. 2. Covariance of gradients of the global energy function with respect to translation and rotation motion of individual slices for the initially misaligned stacks in Fig. 3. A, S and C represent axial, sagittal and coronal slices, respectively. Grid lines are added for better reading.

In this experiment, Levenberg-Marquardt method is used,

$$\Theta^{k+1} = \Theta^k - [2(\nabla_\Theta D)^\top \nabla_\Theta D + \alpha I]^{-1} \nabla_\Theta E, \tag{4}$$

where $\nabla_\Theta E = 2(\nabla_\Theta^\top D)^\top D$. The partial derivative of D with respect to a specific component θ' in Θ is an analytical function:

$$\frac{\partial D}{\partial \theta'} = \sum_{i,j} \left(\frac{\partial \mathbf{x}_{ij}}{\partial \theta'} \right)^\top \nabla_{\mathbf{x}_{ij}} D. \tag{5}$$

The first order approximation of the Hessian matrix is a covariance matrix that represents the correlation between motion parameters in terms of the variation in D. Figure 2 shows one such covariance matrix, where a translational motion of a slice is either positively or negatively correlated with slices in its orthogonal stacks. Other intuitive correlations between slices can be identified, such that all the entries in rotational-Z vs rotation-Z are negative, which visualizes a bevel gear-like connection between two slices.

The registration procedure is initialized by first estimating a global rigid transformation between the axial and the sagittal, and the axial and coronal stacks [12]. This provides an approximate starting point of the refinement of individual slice locations. From the initial estimation, the update (4) is evaluated. This is repeated according to the current estimation of motion parameters of all the slices, until the decrease

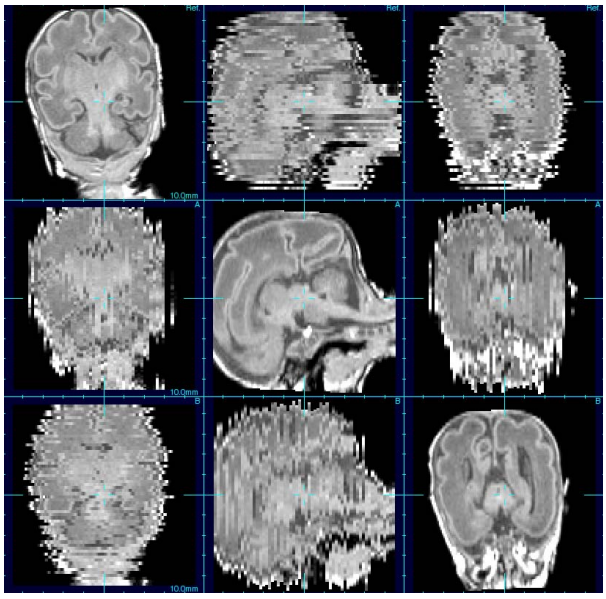

Fig. 3. Three slice stacks with a resolution of $0.7\times0.7\times1.5$ mm^3 with similated motion corruption, displayed row-wisely. Uniform random motion artifacts of [-3,3] mm of translation and [-3,3] degrees of rotation are added to each slice.

in the energy after update is less than a predefined tolerance limit.

3. RESULTS

3.1. Registration of Simulated Misalignment

In order to evaluate the algorithm on representative anatomy with a known ground truth, as in [9] we used T1W 3D SPGR images acquired from a premature neonate of a gestational age of 32 weeks. From this accurate 3D image we extract slices with random location and orientation to simulate a stack of 2D images acquired during fetal motion.

Three orthogonal stacks were generated from the axial stack of the original stack set. The resampling used trilinear interpolation in the original voxel dimensions, namely $0.7\times0.7\times1.5$ mm^3. Simulated random movement was added to each of slices, with [-3,3] mm translation and [-3,3] degrees of rotation. The stacks are shown in Fig. 3.

3.2. Alignment and Reconstruction

The proposed algorithm was implemented, followed by a Gaussian weighted reconstruction as described in [10]. Uniform constrast was assumed in the simulation. The registration error was measured by the root mean square distance between individual voxels from the ground truth. Before the registration, the misaligned stacks had 3.44 mm of RMSE, and after the registration the RMSE was reduced to 1.52 mm.

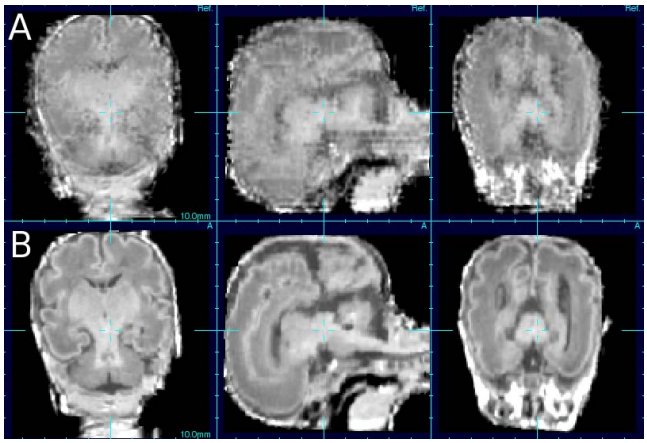

Fig. 4. Comparison of the reconstructed simulation volume (A) before and (B) after the registration.

Fig. 4 depicts the reconstructed volume before the alignment (A), and after the alignment (B). Note the separation between white and gray matter, as well as the sulci structure are improved in (B).

3.3. Registration of Clinical Fetal Image Data

The same procedure was applied to a clinical single-shot fast spin-echo (SSFSE) T2-weighted image set acquired during normal maternal breathing. The sequence parameters were TR=6000 ms, TE effective=90 ms, in-plane resolution 0.5 mm and 3 mm slice thickness. Figure 5 displays axial, sagital and coronal stacks from top to bottom, and the reconstructed volumes are presented in Fig. 6. The volume reconstructed after the slice-wise registration shows sharper edges and stronger constrast (bottom) than one reconstructed with only stack-wise registration (top).

4. DISCUSSION

In this paper, we presented an algorithm to align three orthogonal stacks of MRI slices, where the slices are individually translated and rotated. The proposed approach calculates the correlation of the gradient of mismatch along all the intersections between any two approximately orthogonal slices with respect to rotation and translation of each slice, and then updates the location and the orientation of all the slices at once. The gradient of mismatches is directly calculated from the knowledge of the spatial gradient of each slice image. Since the covariance matrix has a relatively small dimensionality, the inversion can be computed without an approximation. A benefit of this approach is that any parametric image deformations such as illumination or geometrical distortion can be incorporated in the optimization, which is crucial in 3D volume reconstruction in fetal brain imaging, where a highly accurate estimation of motion and illumination is required.

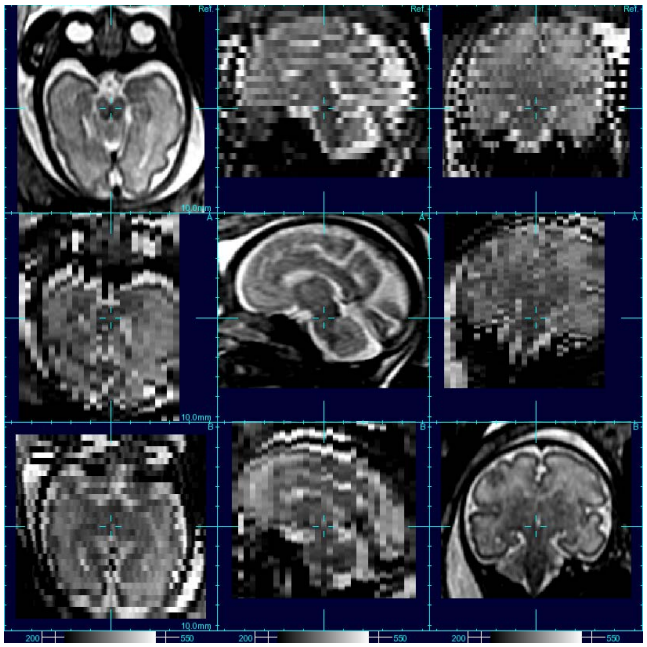

Fig. 5. Axial, sagital and coronal stack of T2 images acquired by SSFSE sequences.

Acknowledgement

This work is primarily funded by NIH Grant R01 NS 055064. The authors would like to thank Dr. Roland Henry for access to image data and advice on the imaging protocols.

5. REFERENCES

[1] D. Levine, "Fetal magnetic resonance imaging," *Journal of Maternal-Fetal and Neonatal Medicine*, vol. 15, pp. 85–94, 2004.

[2] F.V. Coakley, O.A. Glenn, A. Qayyum, A.J. Barkovich, R. Goldstein, and R.A. Filly, "Fetal MR imaging: A developing modality for the developing patient," *American Journal of Roentgenology*, vol. 182, pp. 243–252, 2004.

[3] P.C. Sonigo, F.F. Rypens, M. Carteret, and A. Delezoide, "MR imaging of fetal cerebral anomalies," *Pediatric Radiology*, vol. 28, pp. 212–222, 1998.

[4] C. Garel, E. Chantrel, H. Brisse, M. Elmaleh, D. Luton, J.F. Oury, G. Sebag, and M. Hassan, "Fetal cerebral cortex: Normal gestational landmarks identified using prenatal MR imaging," *American Journal of Neuroradiology*, vol. 22, pp. 184–189, 2001.

[5] N. Girard, C. Raybaud, D. Gambarelli, and D. Figarella-Branger, "Fetal brain MR imaging," *MRI Clinics of North America*, vol. 9, pp. 19–56, 2001.

[6] O.A. Glenn, "Fetal central nervous system MR imaging," *Neuroimaging Clinics of North America*, vol. 16, pp. 1–17, 2006.

[7] P.S. Huppi and T.E. Inder, "Magnetic resonance techniques in the evaluation of the perinatal brain: Recent advances and future directions," In *Seminars in Neonatology*, vol. 6, pp 195–210, 2001.

[8] D. Prayer, P.C. Brugger, and L. Prayer, "Fetal MRI: Techniques and protocols," *Pediatric Radiology*, vol. 34, pp. 685–693, 2004.

[9] F. Rousseau, O.A. Glenn, B. Iordanova, C.E. Rodriguez-Carranza, D. Vigneron, A.J. Barkovich, and C. Studholme, "A novel approach to high resolution fetal brain MR imaging," in *Proc. of Medical Image Computing and Computer Assisted Intervention*, 2005, pp. 548–555.

[10] F. Rousseau, O.A. Glenn, B. Iordanova, C.E. Rodriguez-Carranza, D.B. Vigneron, A.J. Barkovich, and C. Studholme, "Registration-based approach for reconstruction of high-resolution *in utero* MR brain images," *Academic Radiology* vol. 13, pp. 1072–1081, 2006.

[11] S. Jiang, H. Xue, A. Glover, M.A. Rutherford, and J.V. Hajnal, "A novel approach to accurate 3D high resolution and high SNR fetal brain imaging," in *Proc. of IEEE International Symposium on Biomedical Imaging*, 2006, pp. 125–128.

[12] C. Studholme, D.L.G. Hill, D.J. Hawkes, "An overlap invariant entropy measure of 3D medical image alignment," *Pattern Recognition*, vol. 32, pp. 71–86, 1999.

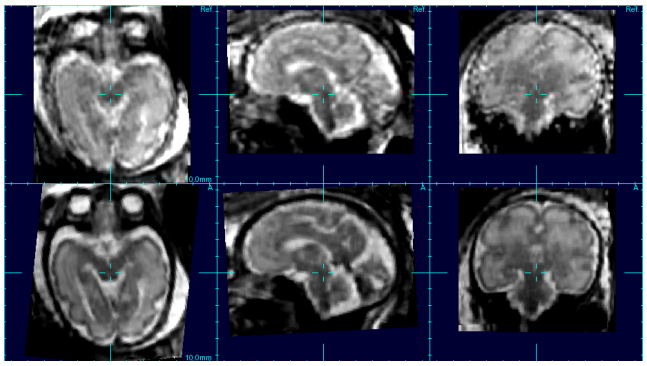

Fig. 6. Comparison of the reconstructed clinical data (A) before and (B) after the registration.